Vibrational spectroscopy as a direct stereochemical probe of polyhydroxylated molecules

F. Passareli,[a] A. N. L. Batista,[a] A. J. Cavalheiro,[a] W. A. Herrebout[b*] and J. M. Batista Junior[c*]

[a]*Institute of Chemistry, São Paulo State University – UNESP, Araraquara, SP 14800-060, Brazil.*

[b]*Department of Chemistry, University of Antwerp, Antwerp B2020, Belgium.*

[c]*Department of Chemistry, Federal University of São Carlos – UFSCAr, São Carlos, SP 13565-905, Brazil.*

Electronic Supplementary Information

Experimental data

Experimental data

Isolation

The dried and powdered leaves of *Cryptocarya mandioccana* (1.0 kg) were extracted with ethanol (glass distillated) in ultrasonic bath for one hour and left to macerate for one day. It was then filtered and the solvent evaporated under reduced pressure. This procedure was performed three times. The ethanolic extract (197.0 g) was dissolved in MeOH/H_2O (9:1, v/v) and then partitioned with hexane (Hex) and ethyl acetate (EtOAc), sequentially.

The EtOAc portion (76.4 g) was fractionated using solid phase extraction on silica gel 60 (63-200 µm, Sigma, 760 g, 10.0 cm x 10.0 cm), and eluted with a gradient of hexane, ethyl acetate and methanol affording the following fractions: F1-Hex (100%) 15.7 mg, F2-Hex/AcOET (95:5) 11.0 mg, F3-Hex/AcOET (90:10) 90.8 mg, F4-Hex/AcOET (80:20) 0.56 g, F5-Hex/AcOET (60:40) 1.05 g, F6-AcOEt (100%) 8.94 g, F7-AcOEt/MeOH (95:5) 13.8 g, F8-EtOAc/MeOH (80:20) 37.6 g, F9-AcOEt/MeOH (60:40) 14.5 g, F10-MeOH (100) 2.78 g, and F11-MeOH/H_2O (1:1) 1.57 g.

Fraction F6 (1.0 g) was submitted to a clean-up procedure on C18 silica gel column (40-60 µm, LiChroprep® RP-18 Merck, 10 g, 2.0 x 5 cm) eluted with MeOH/H_2O (50:50). After that, the separation was carried out on a Phenomenex Luna® C18 HPLC column (250 x 21.2 mm, 10 µm) eluted isocratically with MeOH/H_2O 44:56 (v/v) at a flow rate of 10.0 ml.min^{-1}. Compounds **1** (100 mg; $[\alpha]_D$ −71.4, *c* 1.8 MeOH), **2** (100 mg; $[\alpha]_D$ −30.0, *c* 1.8 MeOH) and **3** (70 mg; $[\alpha]_D$ +55.9, *c* 0.58 MeOH) were isolated.

Fraction F8 (18.8 g) was submitted to silica gel 60 column chromatography (40-63 µm Sigma, 180.0 g, 4.4 x 25 cm), and eluted with Hex/EtOAc/MeOH (60:32:08, 3 L), Hex/EtOAc/MeOH (50:40:10, 2 L), EtOAc/MeOH (80:20, 1 L) and MeOH (1 L) affording 70 subfractions (75.0 mL). Subfraction F8CC22-25 (813.4 mg) was submitted to preparative HPLC in resulting in the isolation of compounds **4** (100 mg; $[\alpha]_D$ −7.62, *c* 1.0 MeOH) and **5** (100 mg; $[\alpha]_D$ +16.4, *c* 0.83 MeOH).

Acetonide Formation

Approximately 10 mg of each styryl-pyrone was dissolved in 2,2-dimethoxypropane followed by addition of catalytic amounts of *p*-toluenesulfonic acid. The reaction was stirred at room temperature for 2-4 h. The organic layer was washed with a saturated solution of $NaHCO_3$ followed by water. The organic layer was then dried under reduced pressure and the resulting acetonides were subject to ^{1}H and ^{13}C NMR analysis. The acetonide from trihydroxylated molecules were purified by preparative thin-layer chromatography in normal phase mode using Hex/AcOEt/MeOH (60:32:08, v/v) as mobile phase, and monitored by UV at 254 nm.

IR and VCD Measurements

IR and VCD spectra of compounds **1**-**5** and their acetonides were recorded with either a Single- or Dual-PEM Chiral*IR*-2X FT-VCD spectrometer (BioTools, Inc.) using a resolution of 4 cm^{-1} and a

collection time of 8-24 h. The optimum retardation of the ZnSe photoelastic modulators (PEMs) was set at 1400 cm^{-1}. Minor instrumental baseline offsets were eliminated from the final VCD spectrum by subtracting the VCD spectrum of each compound from that obtained for the solvent under the same conditions. The IR and VCD spectra were recorded in a BaF_2 cell with 100 µm path length using $CDCl_3$ as solvent for all compounds except **4** and **5**, which were dissolved in methanol-d_4. Samples were prepared using 3-5 mg of each compound dissolved in 150 µL of solvent. The experimental spectra presented in Figure 1 and Figures S1-S5 had their absorption normalized.

Calculations

All DFT calculations were carried out at 298 K in the gas phase using Gaussian 09 software. Calculations were performed for the arbitrarily chosen: (6*S*,2´*S*)- and (6*S*,2´*R*)-**1**; (6*S*,2'*R*,4'*S*)- and (6*S*,2'*R*,4'*R*)-**2.1**; (6*R*,4'*S*,6'*S*)- and (6*R*,4'*S*,6'*R*)-**3.1**. All conformational searches were carried out at the molecular mechanics level of theory with the Monte Carlo algorithm employing the MM+ force field incorporated in HyperChem 8.0.10 software package. Initially, for (6*S*,2´*R*)-**1** and (6*S*,2´*S*)-**1**, 34 and 25 conformers, respectively, with relative energy (rel E.) within 6 kcal mol^{-1} of the lowest-energy conformer were selected and further geometry optimized at the B3LYP/6-31G(d) level. The four and two conformers, respectively, with rel E. <1.4 kcal mol^{-1}, which corresponded to more than 90% of the total Boltzmann distribution, were selected for IR and VCD spectral calculations. Regarding (6*S*,2'*R*,4'*S*)- and (6*S*,2'*R*,4'*R*)-**2.1**, 42 and 48 conformers, respectively, with rel E. within 6 kcal mol^{-1} of the lowest-energy conformer were selected and further geometry optimized at the B3LYP/6-31G(d) level. The four and three conformers, respectively, with rel E. <1.0 kcal mol^{-1} were selected for IR and VCD spectral calculations. Finally, for (6*R*,4'*S*,6'*S*)- and (6*R*,4'*S*,6'*R*)-**3.1**, 31 and 29 conformers, respectively, with rel E. within 6 kcal mol^{-1} of the lowest-energy conformer were selected and further geometry optimized at the B3LYP/6-31G(d) level. During the first conformational search, both chair and twisted boat conformations were probed for the six-membered ring acetonides. The five and four conformers, respectively, with rel E. <1.0 kcal mol^{-1} were selected for IR and VCD spectral calculations. The four lowest-energy conformers identified for (6*R*,4'*S*,6'*R*)-**3.1** were reoptimized and had IR and VCD recalculated at the B3PW91/6-311(d,p) level.

IR and VCD spectra were created using dipole and rotational strengths from Gaussian, which were calculated at the same level used during geometry optimization steps, and converted into molar absorptivities (M^{-1} cm^{-1}). Each spectrum was plotted as a sum of Lorentzian bands with half-widths at half-maximum of 6 cm^{-1}. The calculated wavenumbers were multiplied with a scaling factor of 0.97 for B3LYP/6-31G(d) and 0.99 for B3PW91/6-311(d,p). The final spectra were generated as simple averages of the lowest-energy conformers identified and plotted using Origin 8 software.

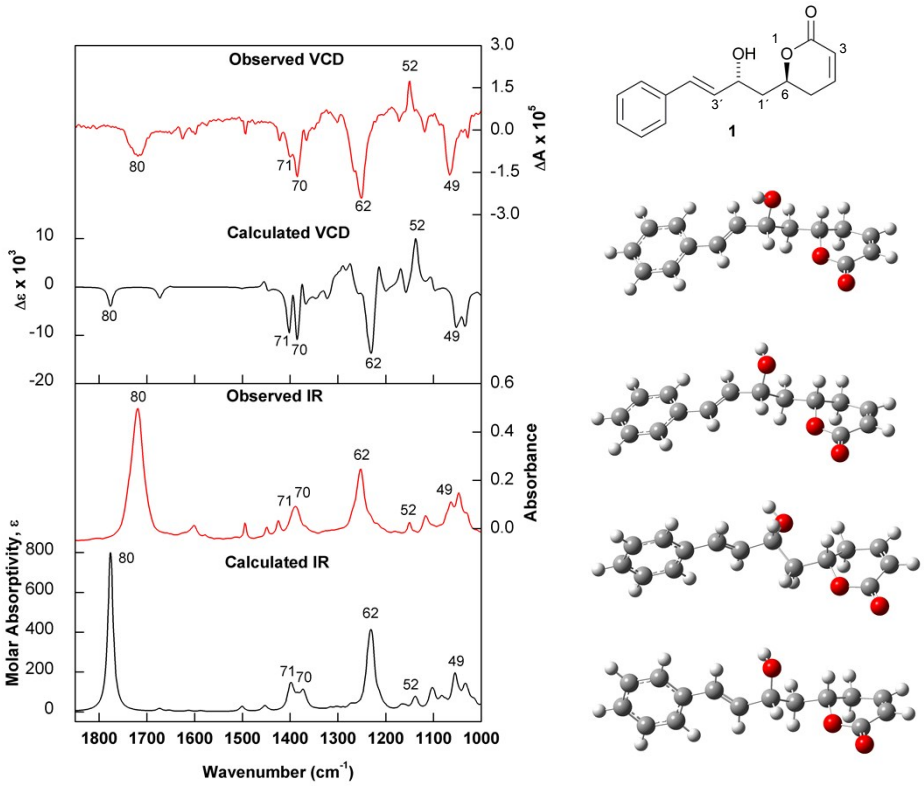

Figure S1. (Left) Comparison of the experimental IR and VCD spectra of deacetylcryptocaryalactone (**1**) with the calculated (B3LYP/6-31G*) IR and VCD spectra of the corresponding (6*S*,2'*R*)-**1**. (Right) Lowest-energy conformers identified for (6*S*,2'*R*)-**1** and used as a simple average.

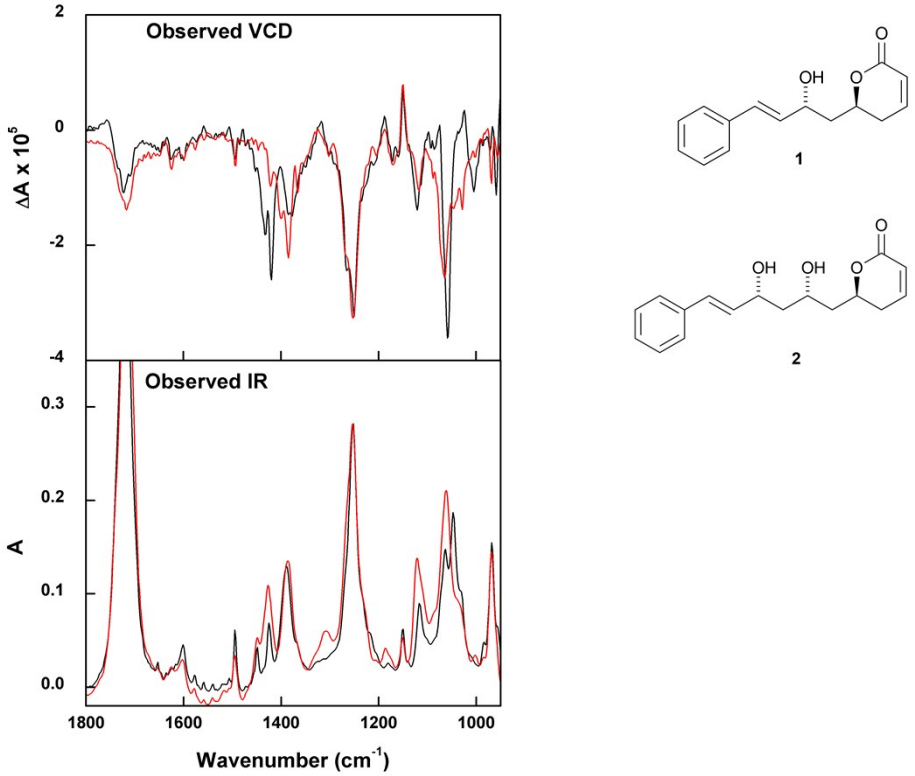

Figure S2. Comparison of experimental IR and VCD spectra of compounds **1** (red) and **2** (black) recorded in $CDCl_3$.

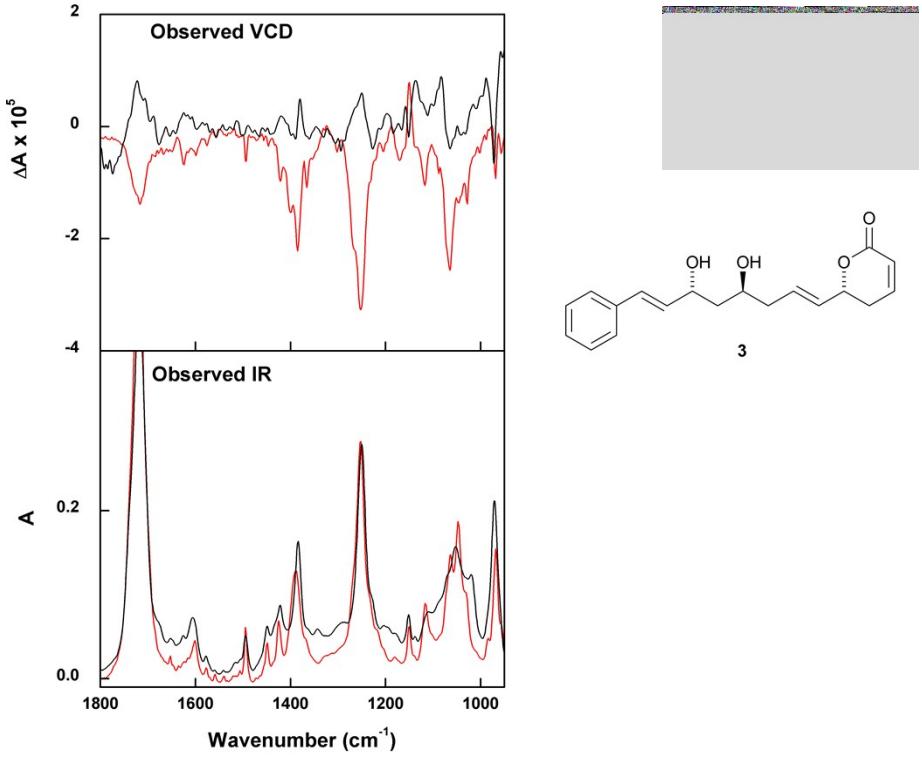

Figure S3. Comparison of experimental IR and VCD spectra of compounds **1** (red) and **3** (black) recorded in $CDCl_3$.

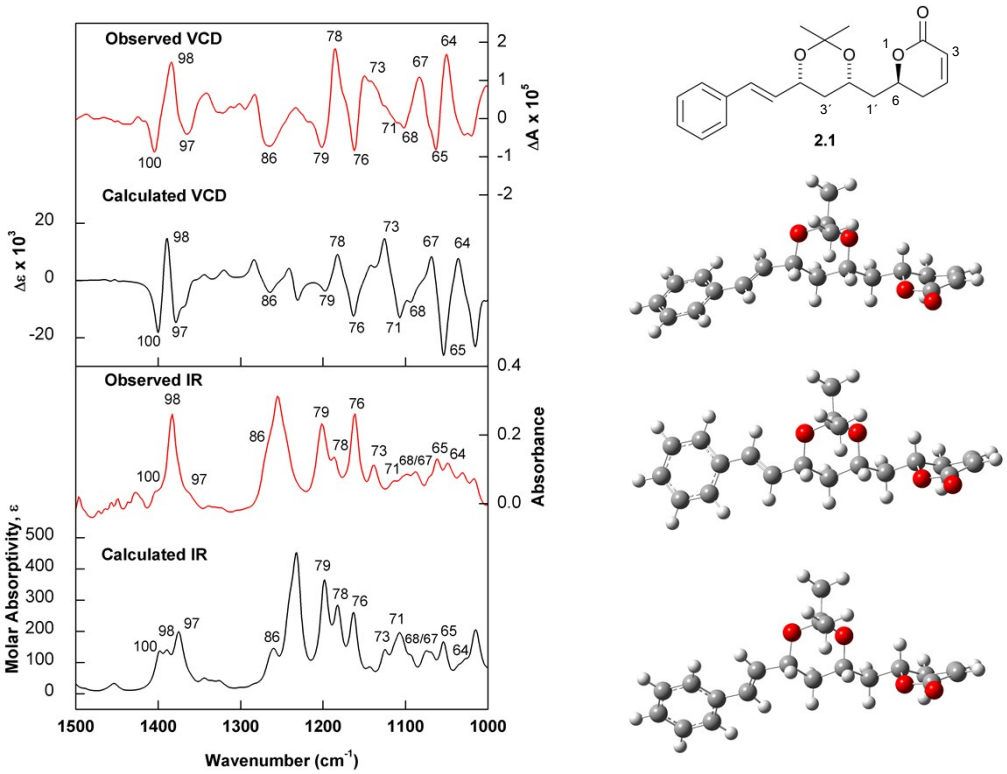

Figure S4. (Left) Comparison of the experimental IR and VCD spectra of compound **2.1** with the calculated (B3LYP/6-31G*) IR and VCD spectra of the corresponding (6*S*,2'*R*,4'*R*)-**2.1**. (Right) Lowest-energy conformers identified for (6*S*,2'*R*,4'*R*)-**2.1** and used as simple average. The priority of the chiral centre at C2'changes according to CPL rules upon creating the acetonide derivative of **2**.

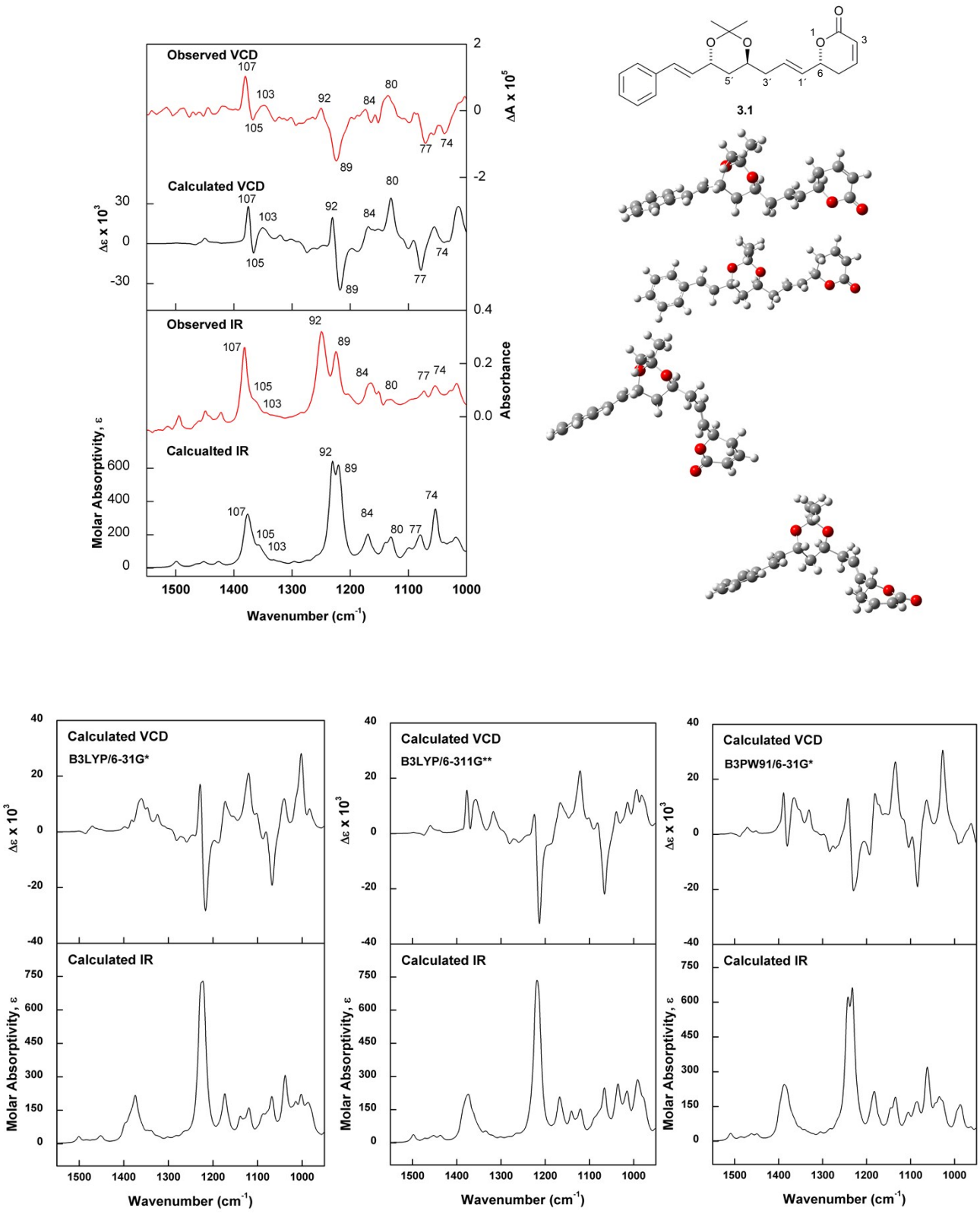

Figure S5. (Top left) Comparison of the experimental IR and VCD spectra of compound **3.1** with the calculated (B3PW91/6-311G**) IR and VCD spectra of the corresponding (6*R*,4'*S*,6'*R*)-**3.1**. (Top right) Lowest-energy conformers identified for (6*R*,4'*S*,6'*R*)-**3.1** and used as simple average. (Bottom) Calculated IR and VCD data, at different levels of theory, for the simple average of the lowest-energy conformers identified for (6*R*,4'*S*,6'*R*)-**3.1**.

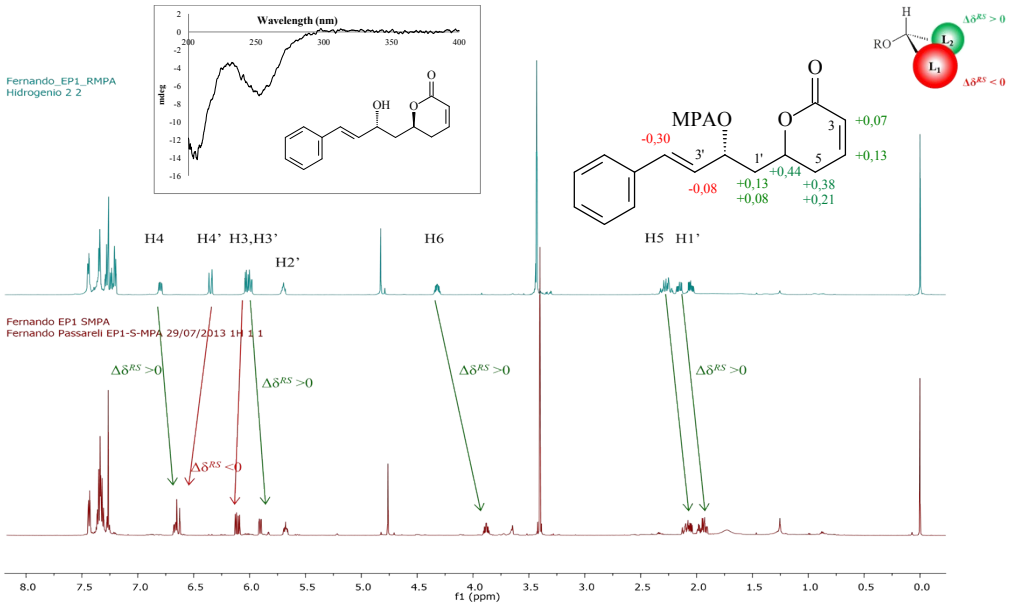

Figure S6. ECD spectrum of compound **1** in methanol; ^{1}H NMR spectra (600 MHz in $CDCl_3$) of (*R*)- and (*S*)-MPA derivatives of compound **1**; Δδ values ($\delta_R - \delta_S$) for the MPA esters in ppm.

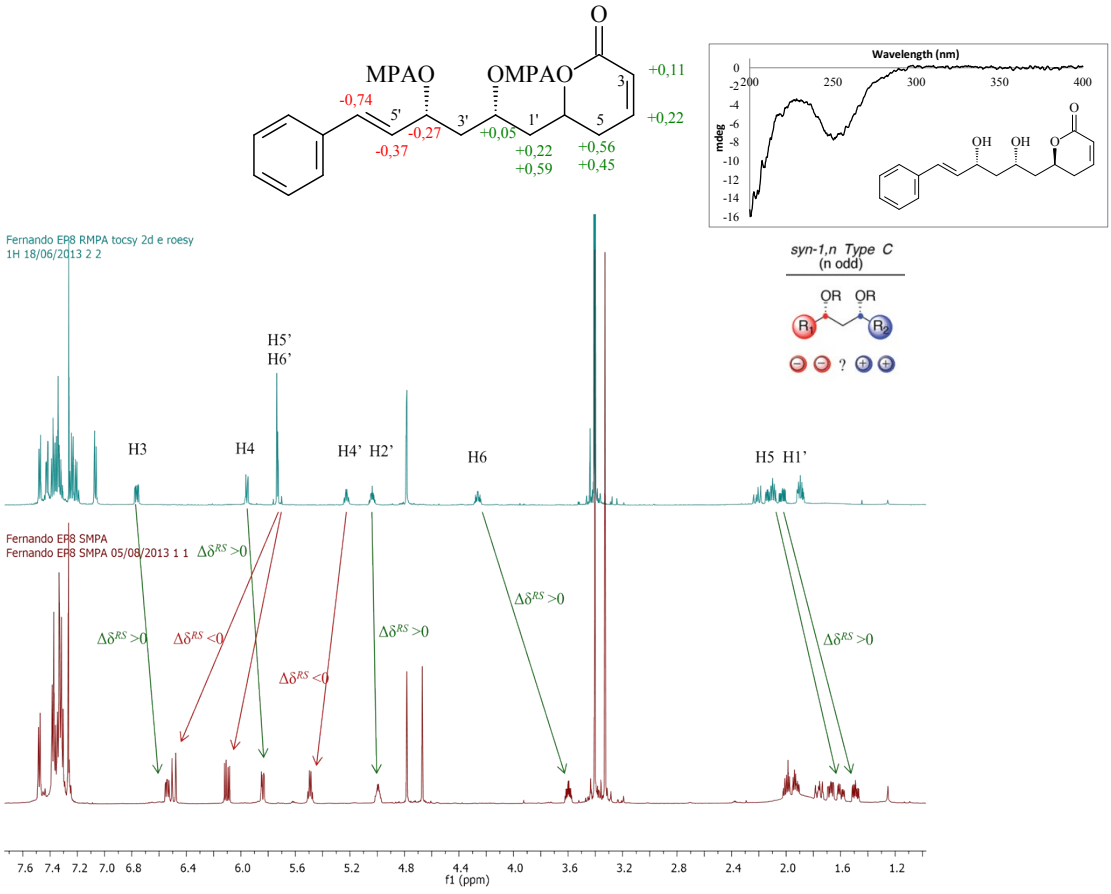

Figure S7. ECD spectrum of compound **2** in methanol; ^{1}H NMR spectra (600 MHz in $CDCl_3$) of (*R*)- and (*S*)-bis-MPA derivatives of compound **2**; Δδ values ($\delta_R - \delta_S$) for the bis-MPA esters in ppm.

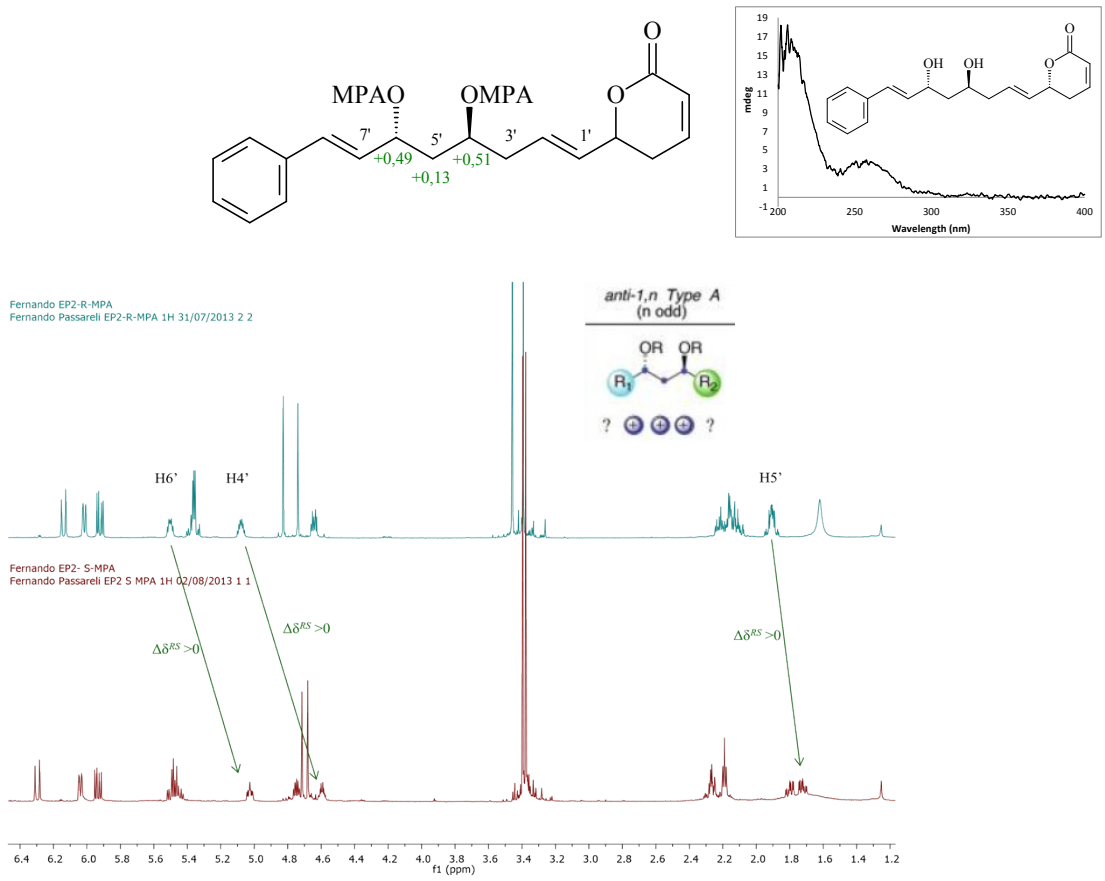

Figure S8. ECD spectrum of compound **3** in methanol; ^{1}H NMR spectra (600 MHz in $CDCl_3$) of (*R*)- and (*S*)-bis-MPA derivatives of compound **3**; Δδ values ($\delta_R - \delta_S$) for the bis-MPA esters in ppm.

Figure S9. ECD spectrum of compound **4** in methanol; ^{1}H NMR spectra (600 MHz in $CDCl_3$) of (*R*)- and (*S*)-MPA derivatives of compounds **4.1** (top) and **4.2** (bottom); Δδ values ($\delta_R - \delta_S$) for the MPA esters in ppm.

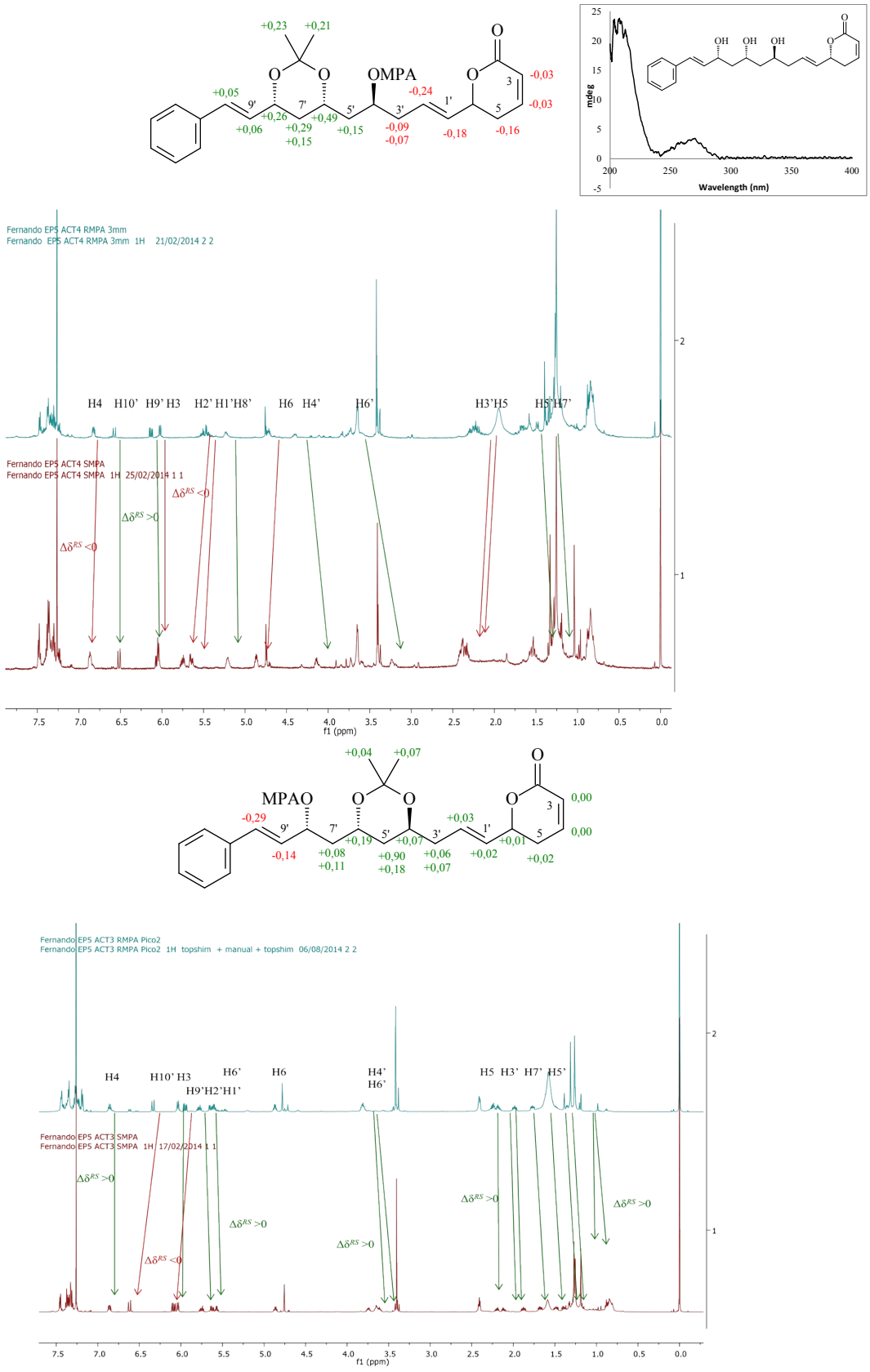

Figure S10. ECD spectrum of compound **5** in methanol; ^{1}H NMR spectra (600 MHz in $CDCl_3$) of (*R*)- and (*S*)-MPA derivatives of compounds **5.1** (top) and **5.2** (bottom); Δδ values ($\delta_R - \delta_S$) for the MPA esters in ppm.